Construction and Dynamics of Knotted Soft Matter Systems

by

Jack Binysh

Thesis

Submitted to the University of Warwick

for the degree of

Doctor of Philosophy

Centre for Complexity Science

....

Contents

Acknowledgments

I acknowledge no one!

Declarations

Replace this text with a declaration of the extent of the original work, collaboration, other published material etc. You can use any LaTeX constructs.

Abstract

Chapter 1

An Introduction to Knotted Fields

1.1 Kelvin's vortex atom

The original, and perhaps most familiar, example of a knotted field is the smoke ring. Easily made by cutting a circular hole in a rectangular box, then replacing the opposite side entirely with a sheet of rubber, "a blow on this flexible side causes a circular vortex ring to shoot out from the hole on the other side" [Thomson, 1867]. In 1867, exactly this demonstration was shown to Lord Kelvin by Peter Guthrie Tait. What is generated is a tightly circulating tube of air, closed into a ring, which propagates stably across the room, rebounding elastically from walls and even other vortex rings (of course to see the ring one first needs to fill the box with smoke, perhaps using dry ice or "a small quantity of muriatic acid" [Thomson, 1867]). At the time, the microscopic nature of atoms was still under debate, and the stability of the rings, a consquence of Helmholtz's laws of vortex motion in an ideal fluid [Helmholtz, 1858] (translated into English by Tait), coupled with their elasticity and capacity for internal vibration [Laan, 2012; Jr., 1996] prompted Kelvin to suggest that "Helmholtz's rings are the only true atoms". Kelvin hypothesised that such rings, embedded in a "perfect homogenous liquid"[1], and "linked together or ...knotted in any manner" might form the microscopic basis of all matter [Thomson, 1867].

Kelvin's "vortex atom" rapidly encountered difficulties in its mathematical content, its falsifiability, and a lack of contempory experimental support [Laan,

[1]Kelvin did not actually specify whether this fluid was the same as the 'ether' hypothesised to transmit electromagnetic waves [Laan, 2012].

a

GLENLAIR
DALBEATTIE,
Nov. 13, 1867.

Dear Tait

If you have any spare copies of your translation of Helmholtz on "Water Twists" I should be obliged if you could send me one.

I set [sic] the Helmholtz dogma to the Senate House in '66, and got it very nearly done by some men, completely as to the calculation, nearly as to the interpretation.

Thomson has set himself to spin the chains of destiny out of a fluid plenum as M. Scott set an eminent person to spin ropes from the sea sand, and I saw you had put your calculus in it too. May you both prosper and disentangle your formulae in proportion as you entangle your worbles. But I fear the simplest indivisible whirl is either two embracing worbles or a worble embracing itself.

For a simple closed worble may be easily split and the parts separated

but two embracing worbles preserve each others solidarity thus

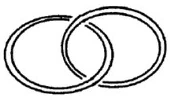

though each may split into many, every one of the one set must embrace every one of the other. So does a knotted one.

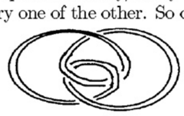

yours truly
J. CLERK MAXWELL

b

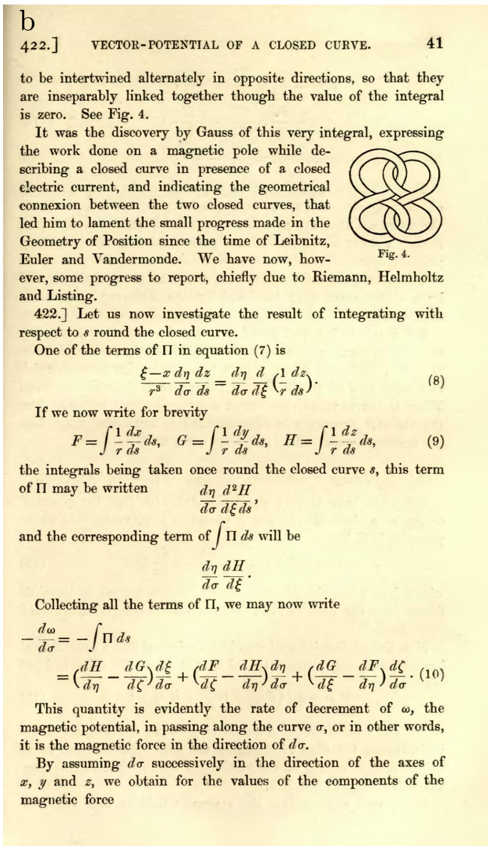

422.] VECTOR-POTENTIAL OF A CLOSED CURVE. 41

to be intertwined alternately in opposite directions, so that they are inseparably linked together though the value of the integral is zero. See Fig. 4.

It was the discovery by Gauss of this very integral, expressing the work done on a magnetic pole while describing a closed curve in presence of a closed electric current, and indicating the geometrical connexion between the two closed curves, that led him to lament the small progress made in the Geometry of Position since the time of Leibnitz, Euler and Vandermonde. We have now, however, some progress to report, chiefly due to Riemann, Helmholtz and Listing.

Fig. 4.

422.] Let us now investigate the result of integrating with respect to s round the closed curve.

One of the terms of Π in equation (7) is

$$\frac{\xi - x}{r^3}\frac{d\eta}{d\sigma}\frac{dz}{ds} = \frac{d\eta}{d\sigma}\frac{d}{d\xi}\left(\frac{1}{r}\frac{dz}{ds}\right). \tag{8}$$

If we now write for brevity

$$F = \int \frac{1}{r}\frac{dx}{ds}\,ds, \quad G = \int \frac{1}{r}\frac{dy}{ds}\,ds, \quad H = \int \frac{1}{r}\frac{dz}{ds}\,ds, \tag{9}$$

the integrals being taken once round the closed curve s, this term of Π may be written

$$\frac{d\eta}{d\sigma}\frac{d^2H}{d\xi\,ds},$$

and the corresponding term of $\int \Pi\, ds$ will be

$$\frac{d\eta}{d\sigma}\frac{dH}{d\xi}.$$

Collecting all the terms of Π, we may now write

$$-\frac{d\omega}{d\sigma} = -\int \Pi\, ds$$

$$= \left(\frac{dH}{d\eta} - \frac{dG}{d\zeta}\right)\frac{d\xi}{d\sigma} + \left(\frac{dF}{d\zeta} - \frac{dH}{d\eta}\right)\frac{d\eta}{d\sigma} + \left(\frac{dG}{d\xi} - \frac{dF}{d\eta}\right)\frac{d\zeta}{d\sigma}. \tag{10}$$

This quantity is evidently the rate of decrement of ω, the magnetic potential, in passing along the curve σ, or in other words, it is the magnetic force in the direction of $d\sigma$.

By assuming $d\sigma$ successively in the direction of the axes of x, y and z, we obtain for the values of the components of the magnetic force

c

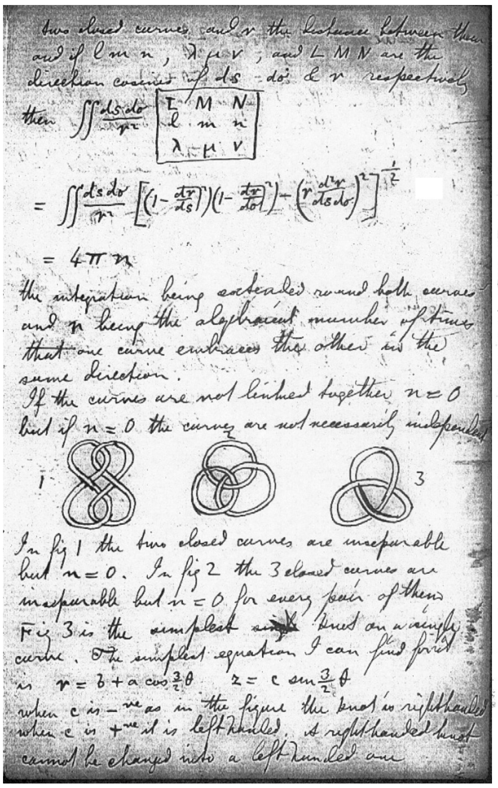

two closed curves and r the distance between them and if $l\ m\ n$, $\lambda\ \mu\ \nu$, and $L\ M\ N$ are the direction cosines of ds $d\sigma$ & r respectively

then $\iint \frac{ds\,d\sigma}{r^2} \boxed{\begin{matrix} L & M & N \\ l & m & n \\ \lambda & \mu & \nu \end{matrix}}$

$$= \iint \frac{ds\,d\sigma}{r^2}\left[\left(1 - \frac{dr}{ds}^2\right)\left(1 - \frac{dr}{d\sigma}^2\right) - \left(r\frac{d^2r}{ds\,d\sigma}\right)^2\right]^{\frac{1}{2}}$$

$= 4\pi n$

the integration being extended round both curves and n being the algebraical number of times ~~that~~ one curve embraces the other in the same direction.

If the curves are not linked together $n = 0$ but if $n = 0$ the curves are not necessarily independent

1 2 3

In fig 1 the two closed curves are inseparable but $n = 0$. In fig 2 the 3 closed curves are inseparable but $n = 0$ for every pair of them. Fig 3 is the simplest ~~sing~~ knot on a single curve. The simplest equation I can find for it is $r = b + a\cos\frac{3}{2}\theta \quad z = c\sin\frac{3}{2}\theta$

when c is $-^{ve}$ as in the figure the knot is righthanded when c is $+^{ve}$ it is lefthanded. A righthanded knot cannot be changed into a lefthanded one

d

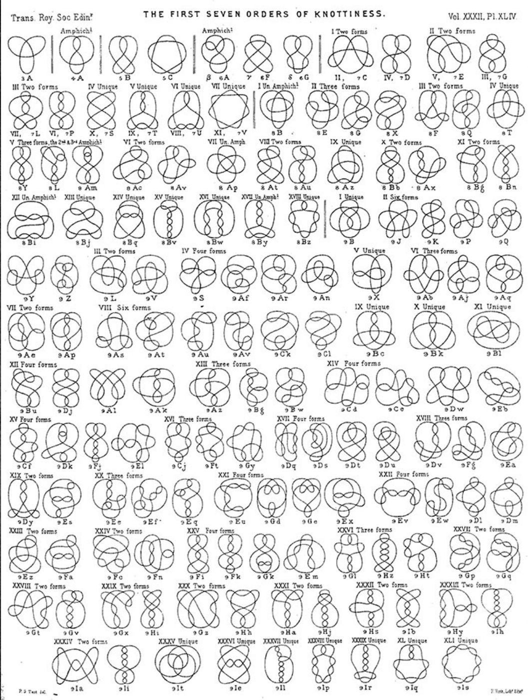

Figure 1.1: hi

2012]. However its content, summarised as "*Physics = Geometry*" in Ref. [Jr., 1996], was compelling (perhaps slightly dangerously so) and apparently motivated Tait, in "consideration of the forms of knots by Sir W. Thomson's (Lord Kelvin) Theory of Vortex Atoms", to construct the first systematic tables of knots in 1876–1885 (Figure 1.1) [Tait, 1876, 1883, 1884]. Tait's articles, alongside a "very remarkable essay by Listing ... and an acute remark made by Gauss ... with some comments on it by Clerk-Maxwell" [**?**]form the initial studies in what is now the mathematical field of Knot Theory Lic. Maxwell himself, although not an active contributor to vortex atom theory, had a clear interest in the ideas, encouraging Tait and Kelvin to "prosper and disentangle your formulae in proportion as you entangle your worbles" (Figure 1.1) [Max]. Indeed the "comments by Clerk-Maxwell" referred to by Tait are in fact Maxwell's rederivation of Gauss's Linking number, as presented in his *A Treatise on Electricity and Magnetsim* in 1873, about which we will have much more to say in **??**.

Despite forming the starting point for modern knot theory, the knotted structures above are quite different to those found in your shoelaces, or in the world of art and design outside the physics department[2]. Rather than a single knotted curve, we have a continuous fluid in whose structure the knot is encoded, and from which dynamical properties of the knot (its motion, stability, a spectrum of vibrational modes etc.) may be derived. More precisely, we have a concentrated tube of vorticity in the fluid, tied into the shape of a knot. Helmholtz's laws of vortex motion demonstrated that, in a perfect (frictionless) fluid this tube of vorticity was 'frozen in' to the fluid, unable to dissapate or cross itself. In an idealised vortex atom, the radius of this tube would tend to zero, with the vorticity contained inside becoming infinite, and we would have a singular linelike structure, tied into a knot and embedded into a continuous three dimensional medium. This structure is our first example of what is called a *knotted field*. There is no strict definition of what constitutes of a knotted field, but a sensible effective one is that they are physical fields containing knotted, linked, or otherwise topologically interesting structure, and that this structure has some interplay with the behaviour of the whole field. As we shall see, such fields are not certainly not confined to fluids.

The disconnect between a knotted curve and a knotted field is reflected in Tait's work, which mentions Kelvin's Vortex Atoms briefly as motivation, but focuses in substance on "*the investigation of the essentially different modes of joining points in a plane*" [Tait, 1876]. As knot theory developed, its initial connections to hydrodynamics and electromagnetism were further abandoned. We also note that

[2]or so I am told.

despite the wonderful knot tables produced by Tait (figure 1.1) and the reliance of vortex atom theory on knotted and linked vortices, there is no mention above of any experimental evidence of vortices tied in nontrivial knots.

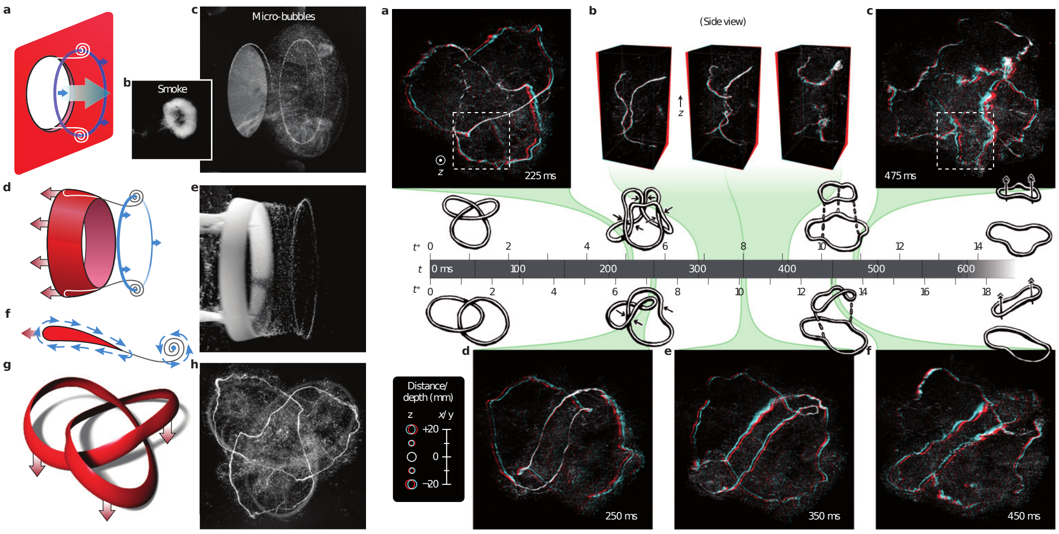

Figure 1.2: hi

The first experimental construction of nontrivial knotted fluid vortices came 140 years after their initial theoretical investigation, from the Irvine lab in 2013 — we show in figure 1.2 several remarkable figures reproduced from Ref. [Kleckner and Irvine, 2013], in which Kleckner et al. tied a single vortex in water into a trefoil knot, the simplest nontrivial knot, as well as linking two vortex loops together (Kelvin's proposed model for a Sodium atom), before tracking their evolution in full 3D. Ref. [Kleckner and Irvine, 2013] is a noteable example of a more general trend; over the past $\sim$ 10 years knotted fields have gone from being purely theoretical constructions to being experimentally realisable in a number of systems, and though originally concieved of in fluid dynamics, modern applications are not limited to this context; they have been realised as nodal lines of optical beams [Dennis et al., 2010], as disclinations in nematic liquid crystals and as spinor Bose-Einstein condensates [Tkalec et al., 2011; Tasinkevych et al., 2014; Čopar et al., 2015]. In the next section we will review the state of modern experiment and theory on knotted fields, beginning with fluids and superfluids — in some sense the most developed case — before moving on to parallel developments in liquid crystals and excitable media, which directly underlie the work in §§**??** and §§**??** in this Thesis. We shall see that the subject has broadened considerably since Kelvin's atoms and the study of fluids. There will be a commonality of ideas between the different disciplines mentioned above, but also geniuine differences.

1.2 Modern knotted fields: Fluids

With the decline of Kelvin's vortex atom theory and the development of knot theory away from its hydrodynamic origins, a resurgence of interest in knotted fields might be dated to the years 1958-1969, with Moreau and Moffatt's seminal papers on Helicity in ideal fluids **??**, preceded by analogous results in magnetohydrodynamics by Woltjer **?**. Focusing on the ideal fluid, both Moreau and Moffatt independently demonstrated that the Helicity

$$\mathcal{H} = \int \mathbf{u} \cdot \boldsymbol{\omega} \; d^3\mathbf{r}, \tag{1.1}$$

where $\mathbf{u}(\mathbf{r}, t)$ is the fluid velocity and $\boldsymbol{\omega} = \nabla \times \mathbf{u}$ is the vorticity **?**, is conserved under the Euler equations of ideal flow. Moffatt in particular gave this invariant a topological interpretation: it measures the linking of vortex tubes within the fluid. Given a fluid where ω is concentrated along discrete sets of curves C_i, Moffat showed that

$$\mathcal{H} = \sum_{i,j,i \neq j} Lk(C_i, C_j)\Gamma_i\Gamma_j \tag{1.2}$$

where Γ_i is the vorticity flux of along curve C_i, and $Lk(C_i, C_j)$ is the Gauss Linking number between curves C_i, C_j (this interpretation of Helicity actually extends to the case where the vorticity is not concentrated along a finite set of curves, but is distributed throughout the fluid **???**). Figure 1.3 shows several examples of vortex tubes with different linking numbers and hence helicities. Seen in this light, the conservation of Helicity is a direct consequence of Helmholtz's laws of vortex motion, and is equivalent to the statement that initially linked vortex tubes remain so; in some sense it is remarkable that the result was not known to Kelvin and Maxwell.

When vorticity is not concentrated along a singular curve but distributed in a thin vortex tube, there is additional internal structure — one imagines a knotted ribbon (Figure 1.4(a)), or rubber bicycle tyre (Figure 1.4(b)). Flux lines may wind around the centre-line of this tube as in Figure 1.4(b), endowing it with a second linking number, the Self-Linking number, which measures the linking of any flux line with the curve centre-line, or equivalently the number of rotations any flux line makes as we traverse the centre-line once. Incorporating this structure into the

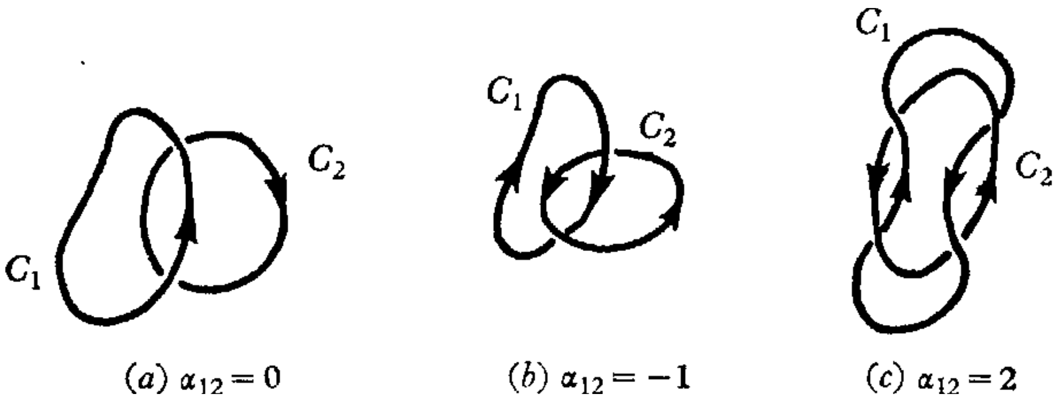

Figure 1.3: hi

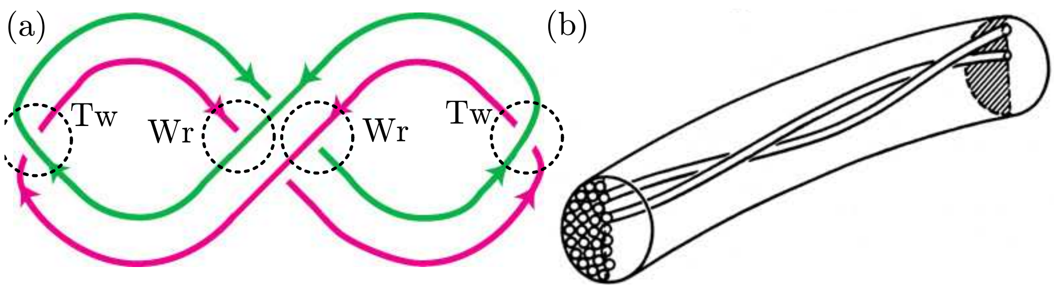

Figure 1.4: hi

helicity count we find **?**

$$\mathcal{H} = \sum_{i,j,i\neq j} Lk(C_i, C_j)\Gamma_i\Gamma_j + \sum_i \Gamma_i^2 SL(C_i) \tag{1.3}$$

where $SL(C_i)$ denotes the self linking of each curve C_i with its implicitly assumed ribbon.

1.2.1 Calugareanu's Theorem, Real fluids

Given a ribbon diagram like figure 1.4(a), the self linking number of may be further decomposed as

$$SL = Tw + Wr. \tag{1.4}$$

The first term, the twist Tw, counts the local crossings of the ribbon over its centre-line. The second term, the writhe Wr, counts non-local crossings of the ribbon over distant parts of the centre line. In figure 1.4 each crossing of the ribbon over its centre-line is annotated with the nature of its contribution. Note that the Wr count is actually independent of the choice of ribbon. For different diagrams of the same knotted ribbon each of these contributions varies, but their sum SL does not. Averaging over also possible diagrams, i.e. all possible projections of the geniuine three-dimensional curve, one obtains integral formulae for twist and writhe, and in this form the result eq. 1.4 was first discovered by Georges Calugareanu **?** (the interpretation of it given above is however due to Ref. **?**). Calagareanu's Theorem is an important and influential result, finding application in Mathematics, Physics, Biology and beyond. It is of potential relevance whenever one studies the properties of a curve with some internal structure, and so it naturally appears frequently in the study of knotted fields. It will play a role in the curve dynamics studied in §§**??** and, in its close connection to Maxwell and Gauss's work on linking numbers and electromagnetism, in §§**??** as well. For the purposes of the current discussion it enables us to speak of *writhe* helicity and *twist* helicity, two seperate contributions to the total helicity count.

In a real (viscous) fluid, helicity is not *a priori* conserved. The question of whether it is in practice, and the mechanism of its dissipation, are areas of active research and motivation for the experiments shown in Figure 1.2 **?**. The reconnections shown in figure 1.2 suggest that helicity is not conserved, however experiments tracking its evolution in detail **???** find that this is not the case. Instead, reconnections transfer the initial linking of curves (c.f. eq. 1.3) into self linking, preserving total helicity to a remarkable extent. More precisely, what is conserved is the sum $Lk + Wr$, with the helicity in Lk being transferred to Wr at a reconnection; the twist helicity Tw is dissipated by viscosity (figure 1.5).

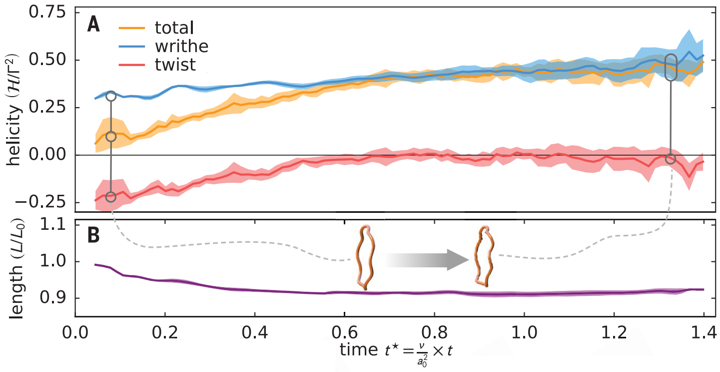

Figure 1.5: hi

1.2.2 Fluids as a case study

The hydrodynamic (and magnetohydrodynamic) story of knotted fields is well developed. We have given a sketch, but the reader is invited to find more detail in reviews such as Refs. **??**. Outside of hydrodynamics the above discussion acts as a template for what one might expect in knotted fields more generally; a test case which other systems may be compared to and contrasted against. In particular, linking and self-linking of structure occur in a variety of contexts, and in an analogy to (1.3) one might seek to connect them to conserved quantites, and use them to understand the dynamics of the entire system under study. To give a brief example of system for which this template is fruitful consider superfluids, close cousins of normal fluids described by a complex scalar field $\psi = |\psi|e^{i\phi}$ (Figure 1.6(a)) evolving via the non-linear Schroedinger equation **?**. Here vortices are given by singular lines where the circle-valued phase field ϕ is undefined, and about which it winds by 2π. As in fluids, one may define some notion of helicity (although its precise form is more ambiguous than is the case in fluids **?**), initialise knotted vortices and study their evolution (figure 1.6(b)) **?**. The helicity evolution turns out to be remarkably similar to that of real fluids **?**; reconnections occur in a manner similar to thse found in real fluids, and they preserve the combination $Lk + Wr$.

However, it is not the case that knotted fields in other systems may be understood simply through the lens of fluids. In the following section we turn to the second experimental system with which substantial work on knotted fields has been done, the nematic liquid crystal cells of Refs. [Tkalec et al., 2011; Tasinkevych et al.,

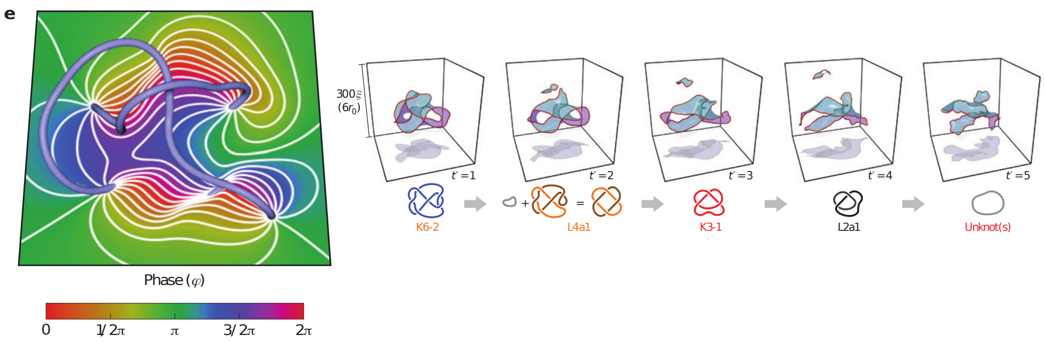

Figure 1.6: hi

2014; Čopar et al., 2015]. There will be some crossover with the discussion above, but also geniuine differences, especially in the theoretical constructions involved, which are of a quite different character.

1.3 Modern knotted fields: Liquid Crystals

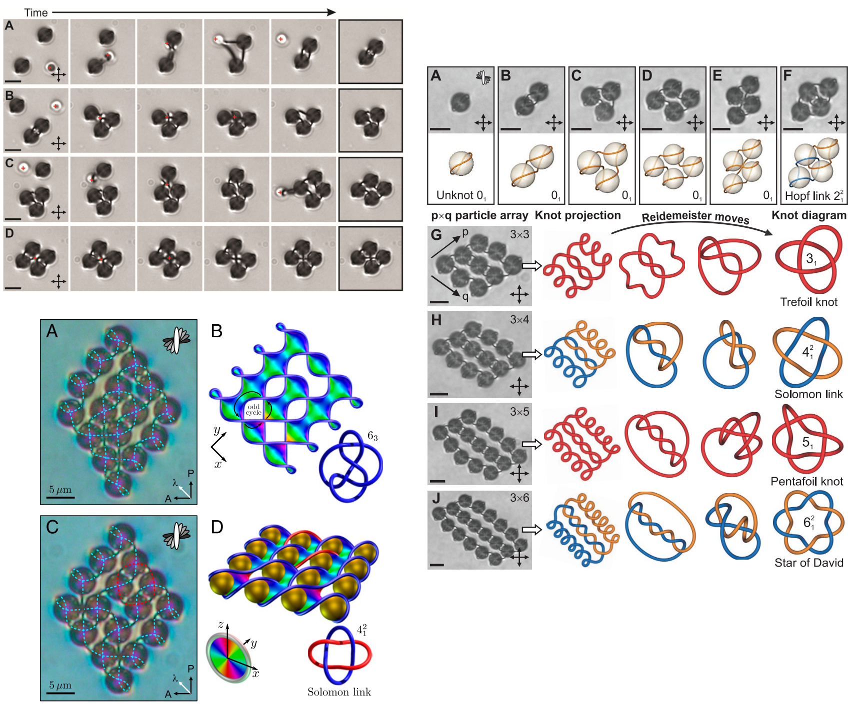

Figure 1.7: hi

A second experimentally constructed knotted field is shown in figure 1.7. It is quite different to that of figure 1.2. By including microscopic colloids a few

μm wide into a thin cell of nematic liquid crystal, experimentalists [Tkalec et al., 2011; Tasinkevych et al., 2014; Čopar et al., 2015] are able to force the appearance of defect lines in the material. These defects may then be manipulated with lazer tweezers, and by weaving them about an array of colloids, a knotted field encoding any type of knot or link can be constructed; unlike the fluid vortices above, these structures are stable, able to be experimentally probed in some detail. This system provides a testbed for series of new ideas about knotted fields described below, but first we step back a moment and provide a brief description of what liquid crystals, defects and colloids etc. actually are.

1.3.1 A brief introduction to liquid crystals

Liquid crystals are a class of materials which possess properties associated to both liquids and solids **?**. In their most common form, the nematic phase, they show no positional order, and flow like a liquid . However, they do show orientational order: if one attempts to twist a portion of the liquid crystal it will respond elastically, as a solid would[3]. The microscopic basis for this behaviour comes from the type of molecules which comprise nematics, two examples of which are shown in Figure 1.8; they are typically thin rods which locally align themselves along some common axis without taking on any sort of crystalline postitional order. In continuum theories this orientational order is described by a spatially varying unit vector field **n**, called the director, which represents an average local molecular orientation, as shown in Figure 1.8 (c).

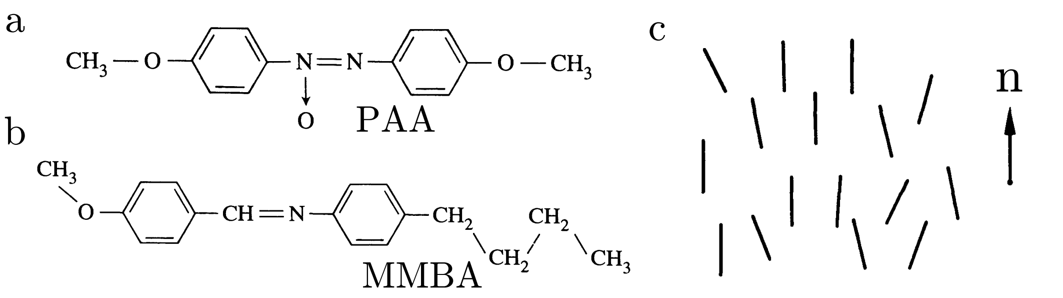

Figure 1.8: hi

The theory of their elastic distortions contains much interesting geometry which we will return to in §**??**, but for an understanding of figure 1.7 we instead focus on a celebrated feature of nematics **?**, their topological defects. If one shines

[3]This is remarkable: imagine your surprise if, upon attempting to stir your coffee, you found it fiercly resisted your attempts to turn the spoon, but was nevertheless happy to be poured down the sink.

polarised light through a thin slice of nematic placed between crossed polarisers, they will observe something like figure 1.9(a), a Schlieren texture **?**. Places in the sample where the director **n** is aligned with one of the two polariser directions H and V do not transmit light, leading to the dark brushes observed. One immeadiately notes points where the brushes meet, sometimes with two brushes leading into a point, sometimes four. What is the structure of the director at these points? The confluence of dark brushes implies that, in a small circle around these points, the director winds, and that at the point itself we cannot consistently define **n**; these points are topological defects, places where the order breaks down. Traversing such a circle around a point with two brushes, the director is aligned with each of H and V only once; in other words it makes only half a turn in a full circle around the defect. This observation is enough to establish that the director **n** must in fact be non-orientable; it should not be thought of as a vector field, but as a line field, for which $\mathbf{n} \sim -\mathbf{n}$. In figure 1.9 (b)–(e) we show configurations of the director

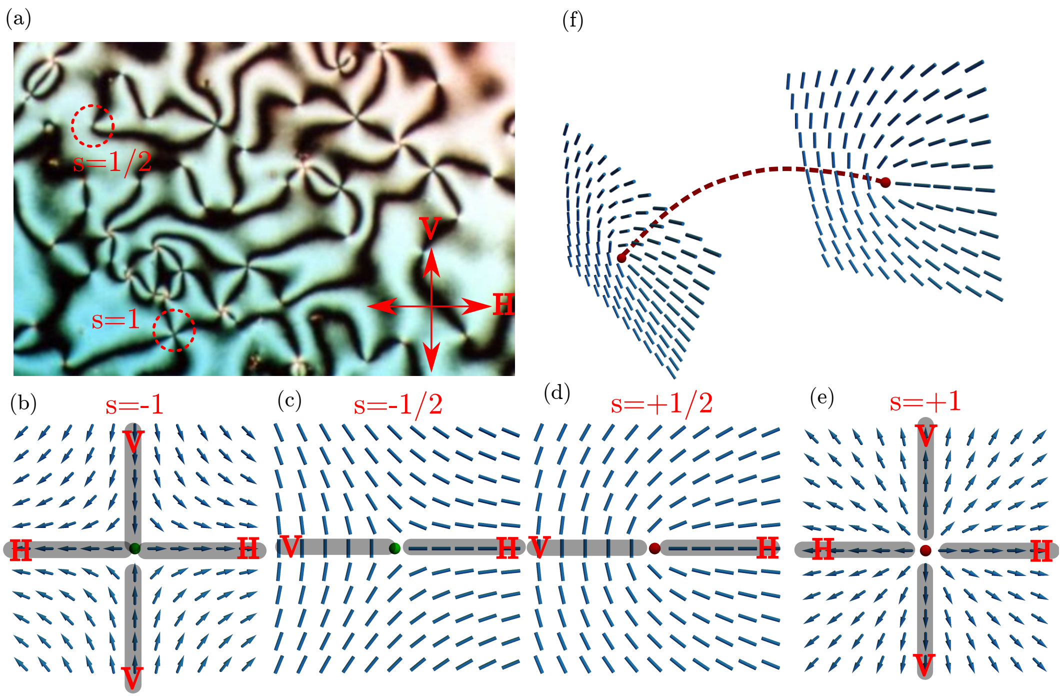

Figure 1.9: hi

around these defects, with their associated Schlieren texture brushes. In (b) and (e) we have four brushes, and a line field which can be oriented; to emphasise this fact we have decorated the line field with one of the two possible choices of arrowheads. Figures (c) and (d) correspond to the non-orientable two brush case; here one cannot consistently assign arrowheads to the rods (it is worth trying to imagine doing so). Note that from a single image such as figure 1.9(a), we cannot distinguish defects winding in a right handed sense (+, in the figure) from left handed by counting brushes. In two dimensions these defects, also called disclinations or dis*in*clinations **?**, are points, but in three dimensions they are lines, transverse cross sections of which have local profiles resembling the two dimensional case; a schematic illustration is shown in Figure 1.9(f). As with fluid vortices, these disclination lines may be knotted and linked together, and the rotation of the local profile along the disclination (see the cross sections in Figure 1.9(f)) provides internal structure giving rise to self linking.

Experiments on knotted disclination lines

We now return to the experiments of Refs [Tkalec et al., 2011; Tasinkevych et al., 2014; Čopar et al., 2015]. In contrast to situation in fluids, one of the major advantages of working with liquid crystal disclinations is the control experimentalists have over them. By including microscopic silica spherical colloids (4.72 μm diamter in figure 1.7) into a sample of liquid crystal with specific surface anchoring conditions, experimentalists may frustrate alignment of the director $\mathbf{n}$ in a controlled fashion, neccesitating the appearance of disclination lines . For example, in a thin cell of liquid crystal treated to promote uniform alignment of $\mathbf{n}$ within the sample, the inclusion of a colloid with normal anchoring conditions forces the appearance of a defect line around it to cancel the colloid's topological charge (it effectively acts as a point defect) and allow $\mathbf{n}$ to relax to uniform at large distances. Two such "Saturn's ring" configurations may be seen in the first frame of figure 1.7(a). Once generated, these disclinations, as well as the colloids they wrap around, may be further manipulated using lazer tweezers [Tkalec et al., 2011], as shown in the remainder of figure 1.7(a). When two of these colloids are brought together the disclinations, either spontaneously or induced by the tweezers, fuse together (Figure 1.7(a), top row). Assembling an array of these colloids and weaving the disclination lines around them, the setup of Refs. [Tkalec et al., 2011; Tasinkevych et al., 2014; Čopar et al., 2015] allows targeted construction of any knot or link; examples of some possible link topologies are shown in Figure 1.7 (b). This system strikingly illustrates that knotted fields have more structure than a single knotted curve; the curve organises the entire field (in this case the director $\mathbf{n}$) around it. Figure 1.7(c) shows the knotted liquid crystal coloured by whether the director is twisting in a right or left handed sense. We see that the disclinations separate the liquid crystal into alternately right and left handed regions. In fact this division allows construction of a surface spanning the disclinations called the Pontryagin-Thom (PT) surface

?, shown as the coloured surfaces in figure 1.7(c), which classifies the topology of this liquid crystal texture; we shall return to it in a moment.

Let us compare the phenomena seen here to §1.2. In contrast to fluid vortices, it is experimentally possible to stabilise liquid crystal disclinations with colloids. This fact alone leads to many differences in the character of theoretical work on them. In the absence of the stabilising colloids, the disclinations will shrink under effective line tension and undergo reconnections, however there is relatively little theoretical work on possible conservation laws analogous to eq. (1.3) or on the structure of these reconnections, although some results do exist **?**. In this sense the dynamics of these knotted fields is less understood than is the case in fluids. It turns out, however, that there is much to be understood even about the statics of knotted liquid crystal fields. Loosely, this may be understood by observing that in a two dimensional fluid there is only one type of vortex, topologically speaking. In a slice of liquid crystal, however, we saw there were many types, indexed by the winding of the director. What of liquid crystal textures in three dimensions? More specifically, given the knotted disclinations shown in figure 1.7, are the liquid crystal textures corresponding to them unique, or are there many inequivalent possibilites ? Questions like these have a long history in liquid crystal physics which, coupled with the difference in experimental possibilites we saw above, makes some split between the character of work on knotted fields in fluids and that in liquid crystals expected.

1.3.2 Homotopy theory of knotted disclinations and Pontryagin-Thom surfaces

The traditional method of understanding liquid crystal textures containing defects is to place a measuring surface around a defect and study the possible textures on this surface, i.e. the different classes of map from the measuring surface to the space of possible values the order takes. Maps are equivalent when a continuous deformation, called a homotopy, exists between them, and as such this framework is known as the homotopy theory of defects **??**. For point defects in a two-dimensional slice of nematic, this is what we did above, using a circle as our measuring surface. There, the space of possible directions $\mathbf{n}$ can point in is $S^1/\{x \sim -x\}$, the circle with antipodal points identified, also called the real projective line $\mathbb{R}P^1$. Thus the different classes of texture are reduced to the classification of maps $\mathbf{n} : S^1 \to \mathbb{R}P^1$. Actually computing these classes is the work of Algebraic Topology, in which maps of a sphere S^n into a space X are termed the homotopy groups $\pi_n(X)$. It is found that $\pi_1(\mathbb{R}P^1) \approx \mathbb{Z}$ and thus there are infinitely many types of point defect in two dimensions as far as the traditional form of the theory is concerned. In three dimensions, the director takes values in $S^2/\{x \sim -x\}$, the sphere with antipodal points identified, also called the real projective plane $\mathbb{R}P^2$. Encircling a disclination line with a measuring loop as shown in Figure 1.10, we compute $\pi_1(\mathbb{R}P^2) \approx \mathbb{Z}_2$, and thus there are precisely two distinct types of disclination[4].

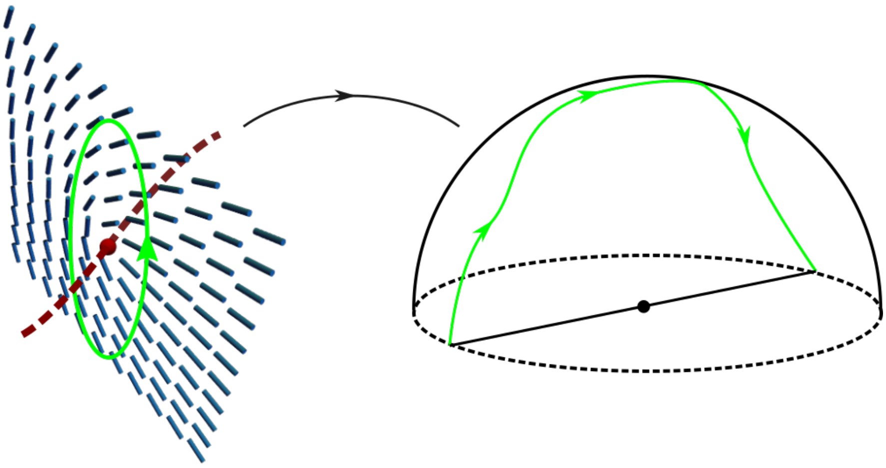

Figure 1.10: hi

A limitation of this approach is that, in only considering the texture on a specific measuring surface (in practice a sphere of some dimension) it discards information about the rest of the texture, which leads to ambiguities when considering multiple defects or more complex structures such as knotted and linked disclinations **??**. A more recent, global approach **?** does not fix a measuring surface, but instead classifies maps into $\mathbb{R}P^2$ where the domain is the entire liquid crystal sample M minus some set of (possibly knotted and linked) disclination lines L. The result is that the homotopy classes of the director are given by

$$[M - L, \mathbb{R}P^2] \approx H_1(\Sigma(L); \mathbb{Z})/\{x \sim -x\} \qquad (1.5)$$

where $\Sigma(L)$ is the branched double cover of the link complement (its appearance in the result is a consequence of director non-orientability), and $H_1(\Sigma(L); \mathbb{Z})$ is its first homology group. Without going into the details of this result, it is clear that these homotopy classes are far richer than the traditional classification scheme for disclinations would suggest, and that they depend strongly on the knot or link under consideration. To illustrate this point, in figure 1.11 we reproduce a 'periodic

[4]One understands this difference by allowing the director in figures 1.9 (b) and (c) to buckle out of the plane of the paper, reducing these textures to the trivial one. This "escape in the third dimension" causes $\mathbb{Z}$ to undergo a mod 2 reduction.

table' of possible textures for (p, q) torus links from Ref. **?**. Taking the simplest example from this table we see that for the Hopf Link, consisting of two curves passing through each other once and given by $(p, q) = (2, 2)$, there are exactly two nonhomotopic textures. Returning to the knots shown in figure 1.7, for each knot there many be multiple nonhomotopic textures, and the knot diagram alone does not tell us which has actually been made. How should we extract this information, and visualise distinct textures? In **??** simple pictures of the director in the vicinty of a defect prove informative, but the same cannot be said of a swarm of sticks in three dimensions.

$p \setminus q$	2	3	4	5	6	7	8	9	10	11	12	13	14	15	16	17	18	19	20
2	2	3	4	5	6	7	8	9	10	11	12	13	14	15	16	17	18	19	20
3	3	2^2	3	1	$\mathbb{Z}^2$	1	3	2^2	3	1	$\mathbb{Z}^2$	1	3	2^2	3	1	$\mathbb{Z}^2$	1	3
4	4	3	$2 \times \mathbb{Z}^2$	5	12	7	$4 \times \mathbb{Z}^2$	9	20	11	$6 \times \mathbb{Z}^2$	13	28	15	$8 \times \mathbb{Z}^2$	17	36	19	$10 \times \mathbb{Z}^2$
5	5	1	5	2^4	5	1	5	1	$\mathbb{Z}^4$	1	5	1	5	2^4	5	1	5	1	$\mathbb{Z}^4$
6	6	$\mathbb{Z}^2$	12	5	$2 \times \mathbb{Z}^4$	7	24	$3 \times \mathbb{Z}^2$	30	11	$4 \times \mathbb{Z}^4$	13	42	$5 \times \mathbb{Z}^2$	48	17	$6 \times \mathbb{Z}^4$	19	60
7	7	1	7	1	7	2^6	7	1	7	1	7	1	$\mathbb{Z}^6$	1	7	1	7	1	7
8	8	3	$4 \times \mathbb{Z}^2$	5	24	7	$2 \times \mathbb{Z}^6$	9	40	11	$12 \times \mathbb{Z}^2$	13	56	15	$4 \times \mathbb{Z}^6$	17	72	19	$20 \times \mathbb{Z}^2$
9	9	2^2	9	1	$3 \times \mathbb{Z}^2$	1	9	2^8	9	1	$3 \times \mathbb{Z}^2$	1	9	2^2	9	1	$\mathbb{Z}^8$	1	9
10	10	3	20	$\mathbb{Z}^4$	30	7	40	9	$2 \times \mathbb{Z}^8$	11	60	13	70	$3 \times \mathbb{Z}^4$	80	17	90	19	$4 \times \mathbb{Z}^8$
11	11	1	11	1	11	1	11	1	11	2^{10}	11	1	11	1	11	1	11	1	11
12	12	$\mathbb{Z}^2$	$6 \times \mathbb{Z}^2$	5	$4 \times \mathbb{Z}^4$	7	$12 \times \mathbb{Z}^2$	$3 \times \mathbb{Z}^2$	60	11	$2 \times \mathbb{Z}^{10}$	13	84	$5 \times \mathbb{Z}^2$	$24 \times \mathbb{Z}^2$	17	$12 \times \mathbb{Z}^4$	19	$30 \times \mathbb{Z}^2$
13	13	1	13	1	13	1	13	1	13	1	13	2^{12}	13	1	13	1	13	1	13
14	14	3	28	5	42	$\mathbb{Z}^6$	56	9	70	11	84	13	$2 \times \mathbb{Z}^{12}$	15	112	17	126	19	140
15	15	2^2	15	2^4	$5 \times \mathbb{Z}^2$	1	15	2^2	$3 \times \mathbb{Z}^4$	1	$5 \times \mathbb{Z}^2$	1	15	2^{14}	15	1	$5 \times \mathbb{Z}^2$	1	$3 \times \mathbb{Z}^4$
16	16	3	$8 \times \mathbb{Z}^2$	5	48	7	$4 \times \mathbb{Z}^6$	9	80	11	$24 \times \mathbb{Z}^2$	13	112	15	$2 \times \mathbb{Z}^{14}$	17	144	19	$40 \times \mathbb{Z}^2$
17	17	1	17	2	17	1	17	1	17	1	17	1	17	1	17	2^{16}	17	1	17
18	18	$\mathbb{Z}^2$	36	5	$6 \times \mathbb{Z}^4$	7	72	$\mathbb{Z}^8$	90	11	$12 \times \mathbb{Z}^4$	13	126	$5 \times \mathbb{Z}^4$	144	17	$2 \times \mathbb{Z}^{16}$	19	180
19	19	1	19	1	19	1	19	1	19	1	19	1	19	1	19	1	19	2^{18}	19
20	20	3	$10 \times \mathbb{Z}^2$	$\mathbb{Z}^4$	60	7	$20 \times \mathbb{Z}^2$	9	$4 \times \mathbb{Z}^8$	11	$30 \times \mathbb{Z}^2$	13	140	$3 \times \mathbb{Z}^4$	$40 \times \mathbb{Z}^2$	17	180	19	$2 \times \mathbb{Z}^{18}$

Table 2.1: $H_1(\Sigma(L))$ for (p, q) torus links with $2 \leq (p, q) \leq 20$. x implies a group $\mathbb{Z}_x$, integer summands are given as usual.

Figure 1.11: hi

One solution is a construction which generalises the dark brushes of Schlieren textures to three dimensions — the Pontryagin-Thom construction **????**. The idea is to extract the set of all points in the sample where the director is horizontal (more generally, perpendicular to some fixed direction in $\mathbb{R}P^2$). This is exactly what a Schlieren textures shows, although Schlieren textures contain some redundancy, showing us the set where the director is both horizontal and vertical — we only really need half this data. In a three dimensional sample this 'horizontal set' is not comprised of lines as in the two-dimensional Schlieren texture but is a surface, the Pontryagin-Thom (PT) surface. After finding this surface, the construction is completed by colouring it according to the orientation in the horizontal plane that the director takes. An illustration of this procedure is shown in figure 1.12(a). A powerful result in Algebraic Topology called the Pontryagin-Thom correspondance **??** shows that these coloured surfaces, taken up to smooth deformations (more precisely framed cobordisms), are in one-to-one correspondance with homotopy classes of maps, and so textures may be visually distinguished by their differing PT surfaces. To illustrate this fact, in figure 1.12(b) we show the two distinct

PT surfaces for the two nonhomotopic Hopf link textures **?** (that they are both a single colour is an indication that representatives from both homotopy classes with the director everywhere in the sample perpendicular to some axis can be chosen). Returning to figure 1.7(c), this construction provides the coloured surfaces shown; by examining the surface and the colour windings upon it, we may place the texture in one of the classes from eq. (1.5). PT surfaces represent an enormous compression of information into a visually immediate form, and their utility is far from limited to disclination lines; we shall use them in our own work in **??**.

PARA ON FLUIDS "impossible to look at these results without feeling that they are of a fundamentally different charcter" linking number vs link determinant. richness of the statics. what happens when the domain changes? floer theory?

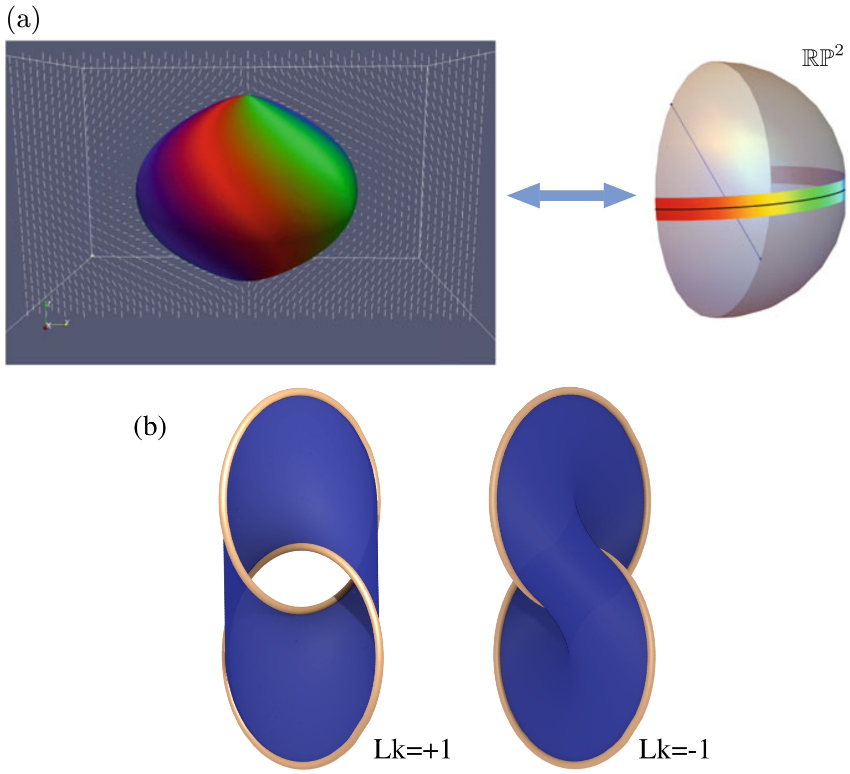

Figure 1.12: hi

1.3.3 Beyond disclination lines

The above sections focused on the knotting and nontrivial topology of disclination lines — defects in the director $\mathbf{n}$ itself. Given the experimental focus on systems of this kind, and their direct connection to the idea of a knotted field, this is natural.

However even in the absence of defects liquid crystals support an array of topological phenomena which may also be considered examples of knotted fields, although perhaps in a different sense to those discussed above.

Skyrmions and Hopfions

The most well known topological feature of this kind is a skyrmion, an example of which is shown in figure 1.13(a) given by the vector field $\mathbf{n}(r) = \cos(\pi r)\mathbf{e}_z + \sin(\pi r)\mathbf{e}_r$ on the unit disk. Fixing the director on the disk boundary, we may wrap this texture around a sphere (compactifying the boundary to a point) at which point its toplogy is captured by a map $\mathbf{n} : S^2 \to S^2$, in other words an element of $\pi_2(S^2) \approx \mathbb{Z}$. These textures are a well studied feature of vector and line fields in two dimensions **?**. We are primarily interested in the properties of order in three dimensions, and as such focus on their three dimensional 'cousins': Hopfions. An experimental image of a Hopfion is shown in figure 1.13(b)**?**. The figure shows a nematic liquid crystal texture inside a three dimensional cell, where the PT surface has been constructed by extracting director orientation via three-photon fluorescence microscopy. What qualifies the Hopfion as a knotted field becomes clear on viewing this surface: each stripe of colour twists about a torus, linking each other colour exactly once — in a Hopf link, no less. Skyrmions are classified by an element of $\pi_2(S^2)$. Hopfions are instead classified by $\pi_3(S^2)$, the third homotopy group of the sphere. Heinz Hopf famously showed that $\pi_3(S^2) \approx \mathbb{Z}$, and in doing so constructed an explicit example of a nontrivial element of this group — the celebrated Hopf Fibration. For mathematical detail on the construction of the fibration we refer to the reader to Refs. **?**, and for an excellent video of its structure we urge the reader to consult **?**. Figure 1.13(b) shows an experimental image of this fibration; the energetics of the liquid system favour a fixed far field nematic direction, mimicking the skyrmion boundary conditions and allowing the domain to be compactified $\mathbb{R}^3 \to S^3$. The nematic texture then realises a map $: S^3 \to \mathbb{R}P^2$, and $\pi_3(\mathbb{R}P^2) \approx \pi_3(S^2) \approx \mathbb{Z}$. The fact that the order lies in $\mathbb{R}P^2$ not S^2 is reflected in that fact that there are two stripes of each colour on the experimental fibration**??**; in figures 1.13(c,d) we show a hopfion in vector order, containing only single stripes, with two particular stripes picked out to make the linking clear.

The geometry of vector fields

The linking of inverse images is the hallmark of the hopf texture (figure 1.13(e)). However without data processing, this linking is not an immeadiately apparent

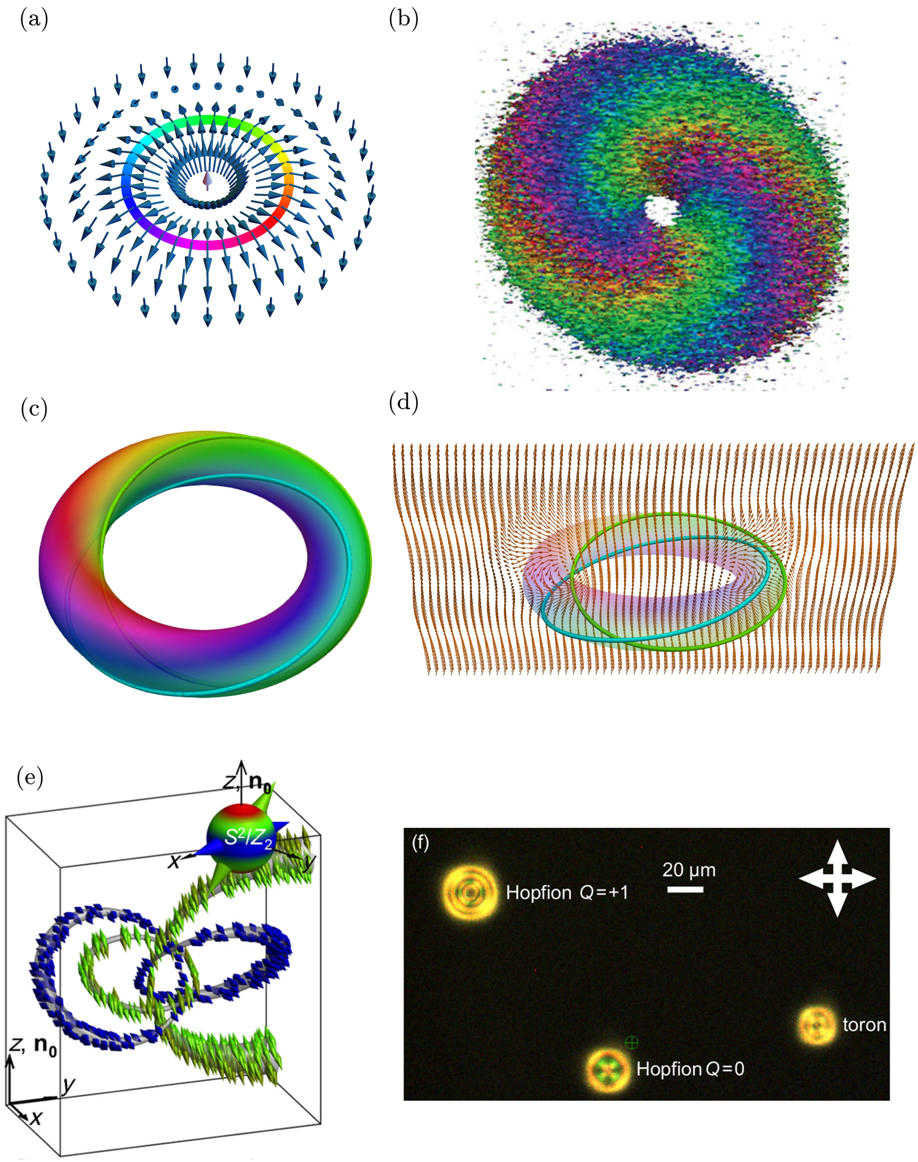

Figure 1.13: hi

feature of the director. By contrast the knotted disclinations, and even their associated PT surface, in figure 1.7 may be clearly visualised. This is a consequence of the coupling of these topological features to the geometry, energetics and ultimately interaction with light of the liquid crystal, a coupling not present in the inverse images charecterising the Hopfion. This observation invites the question: are there 'natural' features of the Hopfion, or nonsingular liquid crystal textures in general, which can be used to infer their topology? We will explore this question, with a particular focus on a recent discovered phase of liquid crystal, in §§**??**. The focus will be on naturally geometric structures inside the liquid crystal which also contain some topological information, and so we now discuss the geometry of liquid crystals, and vector fields more generally.

The fundamental geometry and energetics of nematics was encoded by Frank in 1958**?**, where he gave a free energy for their elastic distortions. We give this free energy here in a slightly nonstandard form, following Ref.**?**:

$$F = \int d^3\mathbf{r} \quad \frac{K_1}{2}(\nabla \cdot \mathbf{n})^2 + \frac{K_2}{2}(\mathbf{n} \cdot \nabla \times \mathbf{n})^2 + \frac{K_3}{2}(\mathbf{n} \cdot \nabla)\mathbf{n} + \frac{K_{24}}{2}\mathrm{Tr}(\Delta)^2, \tag{1.6}$$

where the various K_i are elastic constants[5]. Each term in eq 1.6 comes from a

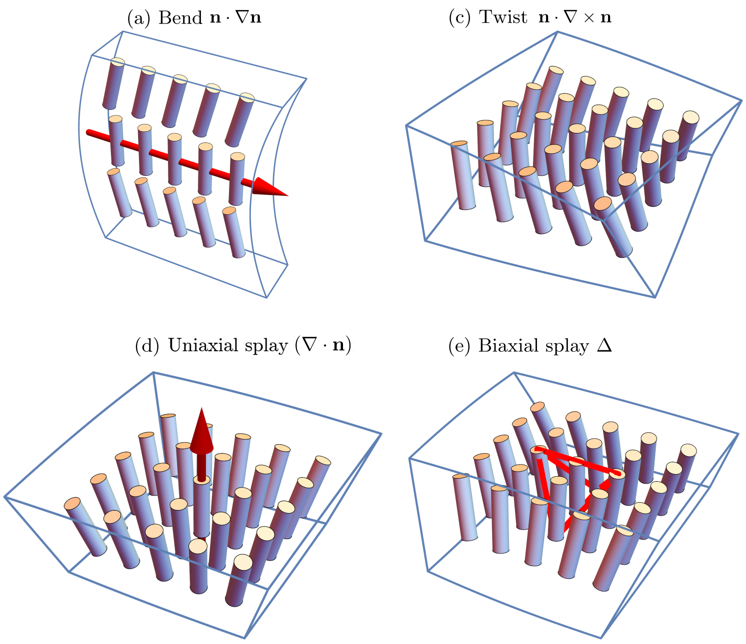

Figure 1.14: hi

[5]These constants do not match one-to-one with those found in the standard writing of the Frank free energy; see Ref. **?**.

different mode of distortion for the liquid crystal, shown in figure (**??**):

$$(\mathbf{n}\cdot\nabla)\mathbf{n} \quad \text{Bend,} \tag{1.7}$$

$$\mathbf{n}\cdot\nabla\times\mathbf{n} \quad \text{Twist,} \tag{1.8}$$

$$\nabla\cdot\mathbf{n} \quad \text{Uniaxial Splay,} \tag{1.9}$$

$$\Delta(\bullet) := \tfrac{1}{2}\Big((\bullet\cdot\nabla\mathbf{n}) + \mathbf{n}\times(\mathbf{n}\times\bullet\cdot\mathbf{n})\Big) \quad \text{Biaxial Splay.} \tag{1.10}$$

Vector order has a local rotational symmetry under which the free energy eq. (1.14) must remain invariant, and indeed the above terms are exactly those combinations of gradients which respect this symmetry. More precisely, the terms appearing in eq. (1.14) correspond to the magnitudes of the irreducible representations of $\nabla\mathbf{n}$ under the action of the rotation group $SO(2)$. These piece together to give a decomposition of $\nabla\mathbf{n}$ which is naturally written in terms of gradients parallel and perpendicular to the director, $\nabla\mathbf{n} = \nabla\mathbf{n}_{\|} + \nabla\mathbf{n}_{\perp}$, where

$$\nabla\mathbf{n}_{\|} = \mathbf{n}^{*}\otimes(\mathbf{n}\cdot\nabla)\mathbf{n} \tag{1.11}$$

$$\nabla\mathbf{n}_{\perp} = \tfrac{\nabla\cdot\mathbf{n}}{2}I - \tfrac{\mathbf{n}\cdot\nabla\times\mathbf{n}}{2}J + \Delta. \tag{1.12}$$

I is the identity transformation, and $J = \mathbf{n}\times\bullet$ is rotation about $\mathbf{n}$.[6]. The geometry of $\nabla\mathbf{n}_{\perp}$ and Δ in particular has been explored in Ref. **?**. $\nabla\mathbf{n}_{\perp}$ describes how $\mathbf{n}$ varies as one moves in a plane perpendicular to it; this is a classical object in differential geometry of surfaces called the shape operator. The decomposition 1.12 corresponds to its breakdown into an isotropic piece I, an antisymmetric piece J and a traceless symmetric piece Δ (if $\mathbf{n}$ were the normal to a family of surfaces the antisymmetric piece would vanish). All directional information is contained in Δ; its eigenvectors coincide with those of $\nabla_{\perp}\mathbf{n}$ and pick out the two directions of principal curvature in plane perpendicular the director. This explains the name 'biaxial splay' for its mode of distortion. The geometry of $\nabla\mathbf{n}_{\|}$ is less well explored. It describes the bending of the director field: if one traces a single curve to which $\mathbf{n}$ is tangent, then $\nabla\mathbf{n}_{\|}$ gives the classical curvature from the differential geometry of space curves **?**. A more complete account of its geometry will in part be the topic §§**??**.

Each of the pieces in 1.12 is manifestly geometric, but they also represent topological information, as canonical sections of vector bundles defined by the director. At each point in the material, the director $\mathbf{n}$ splits the tangent space into a line parallel to $\mathbf{n}$, L_n, and a plane perpendicular to it, ξ, $T\mathbb{R}^3 \approx L_n \oplus \xi$. An example

[6]That the twist and splay terms appear squared in eq. 1.14 is because the decomposition eq. 1.12 is for vector order, not nematic order. The additional symmetry $\mathbf{n}\sim-\mathbf{n}$ forces us to square these terms.

of this splitting is shown in figure 1.15. The families of lines L_n and planes ξ vary smoothly with the director, and such smoothly varying families of vector spaces are called vector bundles . The most famous example of a vector bundle, and the interesting properties they can have, is the family of planes tangent to S^2 (its tangent bundle). The Poincare-Hopf theorem tells us one cannot 'comb a sphere' , in other words one cannot choose a nonzero tangent vector everywhere on the sphere. Said more technically, one cannot find an everywhere nonzero section of the tangent bundle to the sphere. This failure is connected to the topology of S^2; if one sums the windings of all the zeros in the vector field one obtains the Euler Characteristic of S^2. An entirely analogous result holds for any vector bundle; the zeros of a section of a vector bundle encode its Euler Class . Returning to eq. 1.12, $\nabla_\perp \mathbf{n}$ is a section of the bundle $\xi^* \otimes \xi$ — it maps vectors orthogonal to $\mathbf{n}$ into vectors orthogonal to $\mathbf{n}$ — and the bend $\nabla_\| \mathbf{n}$ is a section of the bundle $L_n^* \otimes \xi$. Both probe the topology of ξ and, loosely speaking, as ξ is in one-to-one correspondance with the director $\mathbf{n}$ this topology carries over to $\mathbf{n}$. The zeros of Δ, called umbilic lines in analogy to the umbilic points of the differential geometry of surfaces, have been investigated in Ref. **?**. The zeros of $\nabla_\| \mathbf{n}$, which we will call β lines, will be the subject of §§**??**.

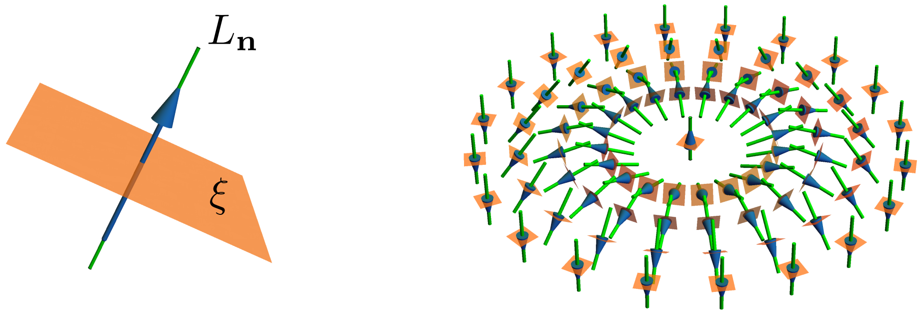

Figure 1.15: hi

The umbilic and β lines are natural geometric structures found in any vector field. However, they assume a particular relevance when strongly coupled to the energetics of the liquid crystal texture. One way to do this is to frustrate the liquid crystal with boundary conditions, as in the disclinations of figure 1.7. Another is to pass to different phase of liquid crystal, where such coupling exists. In the case of umbilic lines, this setting is the cholesteric phase **?**, in which the liquid crystal has a preference for nonzero twist; Δ turns out to be related to the axis of this twisting

?, and its zeros thus encode energetic frustration inside the cholesteric . For β lines, the natural setting is a recently discovered phase of liquid crystal, the twist-bend or splay-bend nematic . These materials, comprised of banana shaped molecules , have an energetic preference for everywhere nonzero bend. A second focus of §§**??** will be on this interplay between geometry and energetics in twist-bend nematics.

1.3.4 Excitable Media

Bibliography

M. R. Dennis, R. P.King, B. Jack, K. O'Holleran, and M. J. Padgett. Isolated optical vortex knots. *Nat. Phys.*, 6:118–121, 2010.

H. Helmholtz. Uber integrale der hydrodynamischen gleichungen, welche den wirbelbewegungen entsprechen. *J. fur die reine und angew Math*, 55:25–55, 1858.

S. J. Lomanaco Jr. The modern legacies of thomson's atomic vortex theory in classical electrodynamics. *AMS Proc. Symp. Appl. MathM*, 51:145–166, 1996.

D. Kleckner and W.T.M. Irvine. Creation and dynamics of knotted vortices. *Nat. Phys.*, 9:253–258, 2013.

S. Van Der Laan. The vortex theory of atoms. Master's thesis, Utrecht University, 2012.

P. G. Tait. On knots i. *Transactions of the Royal Society of Edinburgh*, 28:145–190, 1876.

P. G. Tait. On knots ii. *Transactions of the Royal Society of Edinburgh*, 32:327–342, 1883.

P. G. Tait. On knots iii. *Transactions of the Royal Society of Edinburgh*, 32:493–506, 1884.

M. Tasinkevych, M. G. Campbell, and I. I. Smalyukh. Splitting, linking, knotting, and solitonic escape of topological defects in nematic drops with handles. *Proc. Natl. Acad. Sci. USA*, 111:16268–16273, 2014.

W. Thomson. On vortex atoms. *Proceedings of the Royal Society of Edinburgh*, 6: 94–105, 1867.

U Tkalec, M. Ravnik, S. Čopar, S. Žumer, and I. Muševič. Reconfigurable knots and links in chiral nematic colloids. *Science*, 333:62–65, 2011.

S. Čopar, U. Tkalec, I. Muševič, and S. Žumer. Knot theory realizations in nematic colloids. *Proc. Natl. Acad. Sci. USA*, 112:1675–1680, 2015.